European Journal of Immunology Clinical·Basic·Translational

Immunity to infection

Clinical

Research Article

Plasmodium vivax infection changes the peripheral immunoregulatory network: CD4 T follicular cells and B cells

Natália S. Ferreira[1], Nathália F. Lima[1], Fernando B. Sulczewski[1], Irene S. Soares[2], Marcelo U. Ferreira[1,3] and Silvia B. Boscardin[1]

[1] Department of Parasitology, Institute of Biomedical Sciences, University of São Paulo, São Paulo, Brazil
[2] Department of Clinical and Toxicological Analyses, University of São Paulo, São Paulo, Brazil
[3] Global Health and Tropical Medicine, Institute of Hygiene and Tropical Medicine, NOVA University of Lisbon, Lisbon, Portugal

Regulatory and effector cell responses to *Plasmodium vivax*, the most common human malaria parasite outside Africa, remain understudied in naturally infected populations. Here, we describe peripheral $CD4^+$ T- and B-cell populations during and shortly after an uncomplicated *P. vivax* infection in 38 continuously exposed adult Amazonians. Consistent with previous observations, we found an increased frequency in $CD4^+CD45RA^-CD25^+FoxP3^+$ T regulatory cells that express the inhibitory molecule CTLA-4 during the acute infection, with a sustained expansion of $CD21^-CD27^-$ atypical memory cells within the $CD19^+$ B-cell compartment. Both Th1- and Th2-type subsets of $CXCR5^+ICOS^{hi}PD\text{-}1^+$ circulating T follicular helper (cTfh) cells, which are thought to contribute to antibody production, were induced during *P. vivax* infection, with a positive correlation between overall cTfh cell frequency and IgG antibody titers to the *P. vivax* blood-stage antigen $MSP1_{19}$. We identified significant changes in cell populations that had not been described in human malaria, such as an increased frequency of CTLA-4^+ T follicular regulatory cells that antagonize Tfh cells, and a decreased frequency of circulating $CD24^{hi}CD27^+$ B regulatory cells in response to acute infection. In conclusion, we disclose a complex immunoregulatory network that is critical to understand how naturally acquired immunity develops in *P. vivax* malaria.

Keywords: CTLA-4 · Memory B cells · *Plasmodium vivax* · T follicular helper (Tfh) cells · T follicular regulatory (Tfr) cells

Additional supporting information may be found online in the Supporting Information section at the end of the article.

Introduction

Despite several decades of control efforts and attempts at elimination, malaria remains a major global public health challenge, with 200 million clinical cases and 600,000 deaths yearly, mostly among African children [1, 2]. *Plasmodium falciparum*

Correspondence: Dr. Silvia B. Boscardin and Dr. Marcelo U. Ferreira
e-mail: sbboscardin@usp.br; muferrei@usp.br

is the most prevalent and virulent malaria parasite that infects humans, while *P. vivax* is the most widespread species and predominates outside Africa. Nearly 3.3 billion people are currently at risk of infection with *P. vivax* worldwide and as many as 14.3 million cases are estimated to occur each year [1].

There are several commonalities between the immune responses elicited by human being and experimental murine malaria. Broadly speaking, an early interferon (IFN)-γ response can limit parasite multiplication during the early phase of infection, but cytokines such as interleukin (IL)-10 and transforming growth factor (TGF)-β, released by regulatory T cells (Tregs) and other cell populations, are required to prevent further inflammation and extensive organ damage once parasitemia is under control. Indeed, IL-10-mediated downregulation of T helper (Th) cell responses and CTLA-4 (CD152)-mediated inhibition of costimulation by APCs are major regulatory mechanisms in experimental malaria [3]. CD4 T follicular helper (Tfh) cells play a key role in antibody-mediated protective immunity. They are characterized by the expression of surface molecules C-X-C motif chemokine receptor type 5 (CXCR5 or CD185) and inducible costimulator (ICOS), IL-21 secretion and regulation by the master transcription factor B-cell lymphoma 6 (Bcl-6). CXCR5 expression allows Tfh cells to access lymphoid follicles of the germinal center and direct the production of long-lasting antibodies by providing costimulation to B cells in order to promote class switch recombination, somatic hypermutation, and affinity maturation of antibodies, while ICOS regulates the differentiation of Tfh cells through various signaling pathways. In addition, Tfh cells drive B-cell proliferation by producing IL-21 [4], and those expressing programmed cell death protein 1 (PD-1) are more polarized and highly functional than those negative for PD-1, resembling Tfh cells from germinal centers (GCs) [5]. Different studies have also shown that the Tfh cell compartment is quite heterogeneous, as these cells are able to secrete cytokines characteristic of other subsets of helper T cells [6]. Furthermore, Tfh cell subsets can also be subdivided according to the expression of the chemokine receptors CXCR3 and CCR6 into Th1 ($CXCR3^+CCR6^-$), Th2 ($CXCR3^-CCR6^-$), and Th17 ($CXCR3^-CCR6^+$) [7, 8]. During *Plasmodium falciparum* infection in children, Tfh cells that exhibited a Th1 phenotype were activated primarily, and this activation was not correlated with anti-*Plasmodium* antibody responses [9]. On the other hand, a more recent article by Chan et al. showed that the activation of Tfh cells with a Th2 profile was strongly associated with the functional breadth and magnitude of anti-*Plasmodium falciparum* antibodies [7]. Malaria also induces the expansion of atypical $CD19^+CD10^-CD21^-CD27^-$ memory B cells that may or may not be functionally impaired [10]. Tfh functions are antagonized by specialized T regulatory cells that co-express forkhead box P3 (FoxP3) and CXCR5, known as T follicular regulatory (Tfr) cells, through mechanisms that include CTLA-4-mediated inhibition of B cells and reduced inflammatory cytokine production by Tfh cells following antigenic exposure [11]. IL-10-producing regulatory B cells (Bregs) and plasmablasts ($CD27^{int}CD38^+$) can also dampen T-cell driven immune responses. Bregs comprise two main subsets: $CD24^{hi}CD38^{hi}$ transitional B cells and $CD24^{hi}CD27^+$ cells that are the human equivalent of murine B10 cells [12]. How Tfr and Breg cell subsets respond to human malaria remains little studied [13].

Some critical differences between rodent malaria models—for example, slowly multiplying parasites with tropism for immature red blood cells (RBCs), such as *P. yoelii* XNL, compared to fast-growing parasites with no clear preference for young RBCs, such as *P. chabaudi* AS—may affect immune responses [4]. Not surprisingly, humans also vary in their responses to different malaria parasite species [14]. For example, high levels of proinflammatory cytokines are typically found in both *P. falciparum* and *P. vivax* infections, but IL-10 is consistently expressed at much higher levels in patients with symptomatic *P. vivax* infection, compared to *P. falciparum* [15].

Plasmodium vivax and *P. falciparum* differ in key biological features that are directly relevant to the development of immunity. First, *P. vivax* invades only young $CD71^+$ RBCs called reticulocytes, which account for 1–2% of circulating RBCs in healthy adults [16]; in contrast, *P. falciparum* can infect and multiply within virtually any RBC, either immature or mature. The limited availability of suitable host cells restricts blood-stage multiplication of *P. vivax* and protects naïve hosts from overwhelming parasitemia, as in the *P. yoelii* XNL infection model in mice. Second, the vast majority of RBCs harboring late developmental stages of *P. falciparum* (trophozoites and schizonts) are tightly adhered to the endothelium of capillaries and venules in the brain, spleen, lung, and other organs. Cytoadherence, mediated by *P. falciparum* variant antigens exported to the host cell surface that are targeted by protective antibodies, disrupts blood flow and causes endothelial cell disfunction and local inflammation—the hallmarks of severe malaria [17]. Although cytoadherence can also occur in *P. vivax* infections [18, 19], at levels 10-fold lower than those observed for *P. falciparum* schizont-infected RBCs [18], it is seldom associated with severe organ damage. Third, *P. vivax* originates latent intrahepatic stages that persist for weeks or months and cause parasite relapses when activated. As a result, vivax malaria patients may experience repeated bouts of blood-stage infection, weeks or months apart, following an infectious mosquito bite [20]. Relapses can favor the faster development of immunity to *P. vivax* blood stages, compared to *P. falciparum*, in human populations similarly exposed to primary infections with both species [21, 22].

Compared with *P. falciparum*, immunity to *P. vivax* remains understudied in naturally exposed populations [14]. To address this knowledge gap, we carried out a detailed analysis of effector and regulatory cell populations, including Treg, Tfr, and Breg cells, circulating in the peripheral blood during and shortly after a *P. vivax* infection.

Results

Characteristics of the study population

We analyzed peripheral blood mononuclear cells (PBMCs), plasma, and whole blood from 38 patients aged >18 years with

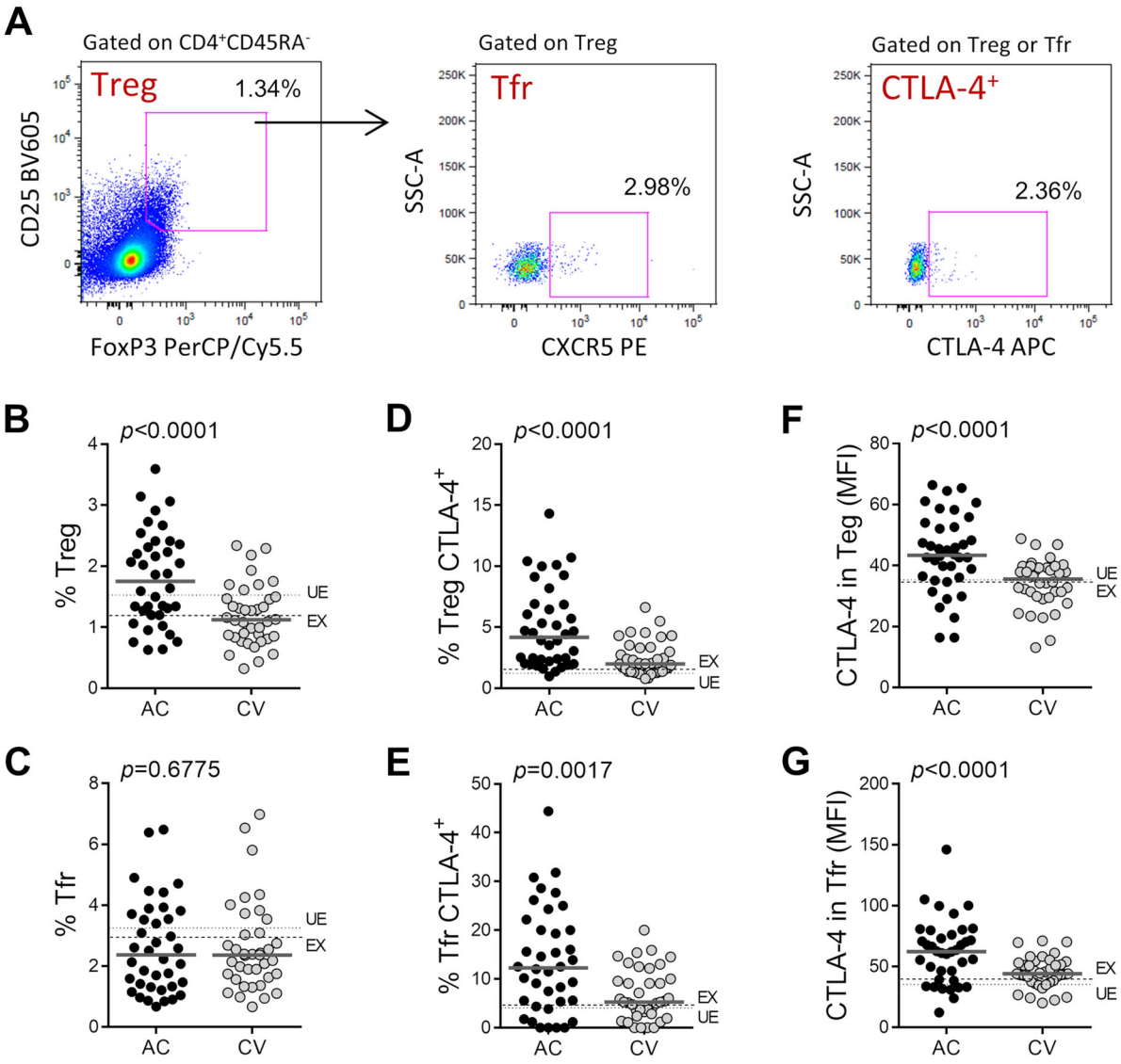

Figure 1. Expression of CTLA-4 on CD4 T regulatory cells and T follicular regulatory cells in response to *Plasmodium vivax* infection. PBMCs from *P. vivax* infected adult patients ($n = 38$) were phenotyped by flow cytometry before (acute-phase sample, AC) and 28 days after starting curative chloroquine-primaquine treatment (convalescence sample, CV). Gating strategy is shown in Supporting information Fig. S6. (**A**) Representative density plots with the frequency of $CD4^+CD45RA^-CD25^+FoxP3^+$ Treg cells (left), $CD4^+CD45RA^-CD25^+FoxP3^+CXCR5^+$ Tfr cells (center), and Treg or Tfr cells that express CTLA-4 (right). Scatterplots show the percentages of Treg cells (**B**) within $CD4^+CD45RA^-$ memory cells and Tfr cells (**C**) within $CD4^+CD45RA^-CD25^+FoxP3^+$, the percentages of Treg and Tfr cells that express CTLA-4 (**D** and **E**) and the median fluorescence intensity (MFI) of CTLA-4 staining on Treg and Tfr cells (**F** and **G**). Horizontal gray lines in scatterplots indicate median values for AC and CV patients. Horizontal dotted lines indicate median values for apparently healthy uninfected controls with similar age and sex distribution who were either malaria-exposed (EX; $n = 40$) or malaria-naïve (UE; $n = 20$). *p* Values for paired comparisons between AC and CV using the Wilcoxon signed rank test are indicated. See Supporting information Fig. S1 and Supporting information Table S2 for comparisons between patient and control groups.

symptomatic but uncomplicated *P. vivax* malaria, sampled before (acute phase, AC) and 28 days after starting treatment with chloroquine-primaquine (convalescence, CV). The median PCR-determined baseline parasitemia was 1361 (interquartile range, 381–2623) parasites/μL. Controls with similar age and sex distribution were 40 apparently healthy malaria-exposed but non-infected (EX), who had remained free of laboratory-confirmed malaria within the past 6 months, and 20 malaria-unexposed (UE) individuals (Supporting information Table S1). Consistent with previous studies (e.g., [15, 23]), we found transiently decreased white blood cell, lymphocyte, monocyte, and platelet counts in AC patients, compared to CV patients and EX and UE controls (Supporting information Table S1).

Increased expression of CTLA-4 on Treg and Tfr cells

In line with previous observations [15, 24, 25], we found a transient expansion of $CD4^+CD45RA^-CD25^+FoxP3^+$ Tregs (Fig. 1A) in *P. vivax* malaria patients, compared with EX controls (Fig. 1B

and Supporting information Fig. S1A; Supporting information Table S2). Tregs accounted for nearly 2% of antigen-experienced $CD4^+$ T cells in AC patients. Moreover, the frequency and expression levels, measured as median fluorescence intensity (MFI), of the key inhibitory molecule CTLA-4 increased in circulating Tregs during the acute infection (Fig. 1D and F and Supporting information Fig. S1A; Supporting information Table S2; see also [15]). CTLA-4 MFIs correlated positively with parasite density (r_s = 0.4213, $p = 0.0084$, data not shown).

We next focused on $CD4^+CD45RA^-CD25^+$ cells that express both CXCR5 and FoxP3, consistent with the Tfr cell phenotype that modulates antigen-specific antibody responses [11]. Circulating Tfr cells did not increase in frequency in response to infection; $CXCR5^+$ cells comprised approximately 2% of the $CD4^+CD45RA^-CD25^+FoxP3^+$ pool in the peripheral blood of adults during and shortly after *P. vivax* infection (Fig. 1C and Supporting information Fig. S1B). However, we observed an increase in the proportions of CTLA-4^+ Tfr cells, with the median levels of CTLA-4 expression by Tfr cells increased by 60–75% during the acute infection compared to EX and UE controls (Fig. 1E and G and Supporting information Fig. S1B; Supporting information Table S2). Moreover, Tfr cells from AC patients expressed significantly higher levels of the costimulatory molecule ICOS, compared to UE controls (Supporting information Table S2). These data suggest that the CTLA-4^+ Tfr cell population may be a significant, yet understudied, modulator of antigen-specific antibody responses elicited by human malaria. Whether CTLA-4 blockade (e.g., with monoclonal antibodies) will affect the ability of Tfr to modulate B-cell proliferation and antibody production remains to be determined.

Th2 polarization of antigen-experienced $CD4^+$ T cells

Next, we examined the $CD45RO^+CD45RA^-$ or memory $CD4^+$ T-cell compartment, which has previously been characterized in other conditions, including in *P. falciparum* infected patients [7, 9]. This cell subset expanded in CV patients, compared to AC patients, but we found no significant differences when CV patients were compared with EX and UE controls (Fig. 2A and Supporting information Fig. S2A; Supporting information Table S3). Within the memory $CD4^+$ T-cell compartment, similar proportions of $CXCR5^+$ and $CXCR5^-$ cells were found in AC versus CV patients (Fig. 2B and Supporting information Fig. S2B and C). Importantly, memory $CD4^+$ T cells were Th2-biased during the infection, with frequencies of the double-negative $CCR6^-CXCR3^-$ (Th2) phenotype increased by 30–65% within the $CXCR5^+$ (Fig. 2C and Supporting information Fig. S2D) and $CXCR5^-$ memory $CD4^+$ T-cell compartments (Fig. 2D and Supporting information Fig. S2E) compared to EX and UE controls (Supporting information Table S3). Simultaneously, there were sustained or transient changes in Th1, Th17, and Th17/Th1 (double-positive) memory $CD4^+$ T-cell frequencies. These data suggest that, under relatively high transmission levels prevailing in our study site [26], *P. vivax* infection in adults selectively induces the expansion of Th2-type antigen-experienced $CD4^+$ T cells.

Changes in circulating Tfh subsets during *P. vivax* infection

Circulating $CD4^+$ $CXCR5^+$ T cells were assumed to be the peripheral counterpart of the germinal center Tfh population, although they downregulate Bcl6 expression upon leaving lymphoid tissue [8]. In our study, the circulating (c)Tfh cell pool was defined as $CD4^+CD45RA^-CD45RO^+CXCR5^+ICOS^{hi}PD\text{-}1^+$, as this phenotype was described as the most closely related to bona fide GC Tfh cells [5]. cTfh cells ($ICOS^{hi}PD\text{-}1^+$) expanded threefold during acute infection and accounted for nearly 5% of the $CD4^+CD45RA^-CD45RO^+CXCR5^+$ cell compartment in AC patients (Fig. 3A and Supporting information Fig. S3A). The magnitude of cTfh expansion correlated positively with baseline parasite density ($r_s = 0.633$, $p < 0.0001$, data not shown). In addition, AC patients differed from EX and UE controls in their relative distribution of cTfh cell subsets (Supporting information Fig. S3B; Supporting information Table S4). The frequencies of Th1 ($CCR6^-CXCR3^+$) and Th2 ($CCR6^-CXCR3^-$) cTfh cells increased by >30% in response to infection, with sustained decreases in Th17 ($CCR6^+CXCR3^-$) cTfh cells and Th17/Th1 ($CCR6^+CXCR3^+$) cTfh cells (Fig. 3B, upper panel). The phenotypically ill-defined $CXCR5^+ICOS^+PD1^+$ and $CXCR5^+ICOS^+PD1^-$ subsets of memory $CD4^+$ T cells did not expand during the infection (Fig. 3A and Supporting information Fig. S3A; Supporting information Table S4). However, the Th2-biased pools of $CXCR5^+ICOS^+PD1^+$ and $CXCR5^+ICOS^+PD1^-$ cells were overrepresented in AC patients, with lower proportions of Th1 and Th17/Th1 cells, compared to EX and UE controls (Fig. 3B, middle and lower panels, and Supporting information Fig. S3B). These results indicate that, under relatively high malaria transmission levels, the less functional Th1 subset [9] and the more functional Th2 subset of cTfh cells [7] are simultaneously induced during *P. vivax* infection in adults.

Antibody titers to the blood-stage antigen $MSP1_{19}$ correlate with cTfh frequency

We measured naturally acquired IgG antibodies to the apical membrane antigen 1 ectodomain (AMA1ect) and to the C-terminal 19 kDa region of merozoite surface protein 1 ($MSP1_{19}$), two vaccine-candidate *P. vivax* blood-stage antigens. Sustained antibody titers to both antigens were found in most patients (Fig. 4A and B); indeed, the majority of patients recognized AMA1ect and $MSP1_{19}$ (Fig. 4C and D). Baseline antibody titers to $MSP1_{19}$ ($r_s = 0.3471$, $p = 0.0328$), but not to AMA1ect (r_s = 0.3026, $p = 0.0648$), correlated positively and significantly with the frequency of cTfh cells (Fig. 4E and F). Among EX controls, who were free of malaria within the past 6 months, antibody titers were substantially lower (Fig. 4A and B). Therefore, titers of

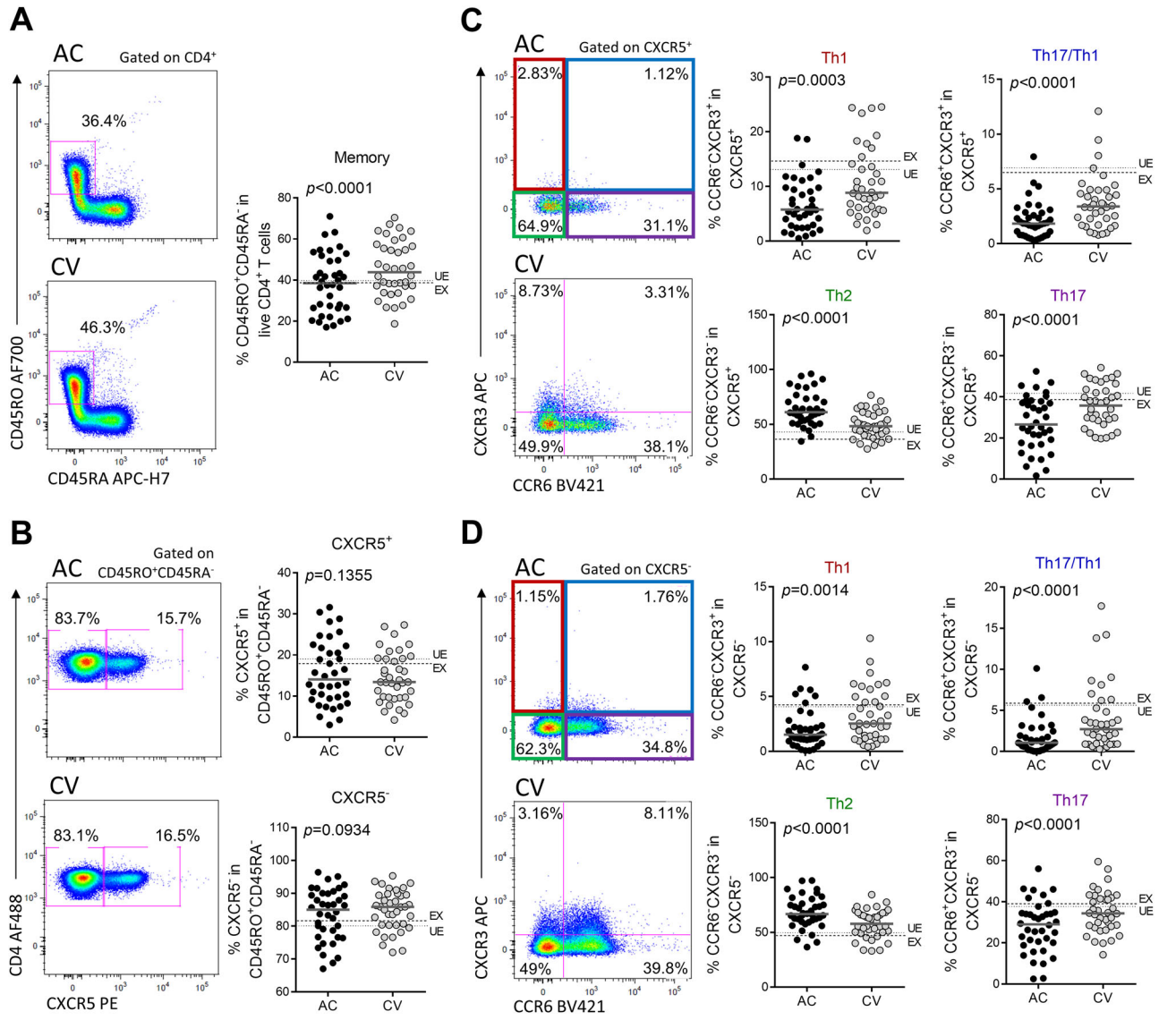

Figure 2. Expression of CXCR5, CXCR3, and CCR6 in the memory CD45RO$^+$CD45RA$^-$ CD4$^+$ T cell compartment in response to *Plasmodium vivax* infection. PBMCs from *P. vivax* infected adult patients ($n = 38$) were phenotyped by flow cytometry before (acute-phase sample, AC) and 28 days after starting curative chloroquine-primaquine treatment (convalescence sample, CV). Gating strategy is shown in Supporting information Fig. S7. (A) Representative density plots (left) and scatterplots (right) showing the percentage of CD4$^+$ T cells with the CD45RO$^+$CD45RA$^-$ memory phenotype. (B) Representative density plots (left) and scatterplots (right) showing the percentages of memory CD45RO$^+$CD45RA$^-$ CD4$^+$ T cells that express or not CXCR5. Representative density plots (left) and scatter plots (right) showing the percentages of CD45RO$^+$CD45RA$^-$CXCR5$^+$ activated memory CD4$^+$ T cells (C) and CD45RO$^+$CD45RA$^-$CXCR5$^-$ memory CD4$^+$ T cells (D) with the Th1 (CCR6$^-$CXCR3$^+$), Th2 (CCR6$^-$CXCR3$^-$), double-positive of Th17/Th1 (CCR6$^+$CXCR3$^+$), and Th17 (CCR6$^+$CXCR3$^-$) phenotypes. Horizontal gray lines in scatterplots indicate median values for AC and CV patients. Horizontal dotted lines indicate median values for apparently healthy uninfected controls with similar age and sex distribution who were either malaria-exposed (EX; $n = 40$) or malaria-naïve (UE; $n = 20$). *p* Values for paired comparisons between AC and CV using the Wilcoxon signed rank test are indicated. See Supporting information Fig. S2 and Table S3 for comparisons between patient and control groups.

specific antibody responses are directly proportional to the frequency of cTfh cells during *P. vivax* infection and decay within the following months in the absence of reinfection.

Sustained expansion of atypical memory B cells

We next evaluated the B-cell compartment in malaria patients. We confirmed some of the previously described changes in the CD19$^+$ B-cell compartment in response to *P. vivax* infection [27–29]. We observed sustained expansions of the CD21$^-$CD27$^+$ activated memory B-cell and CD21$^-$CD27$^-$ atypical memory B-cell pools, as well as transient increases in the proportion of total CD19$^+$ B cells, and CD20$^-$CD21$^-$ plasma cells, with a decreased proportion of CD21$^+$CD27$^-$ naïve B cells during the convalescence (Fig. 5A and B and Supporting information Fig. S4A and B; Supporting information Table S5). There was a transient decrease in the proportion of classical memory CD21$^+$CD27$^+$ B cells, with no change

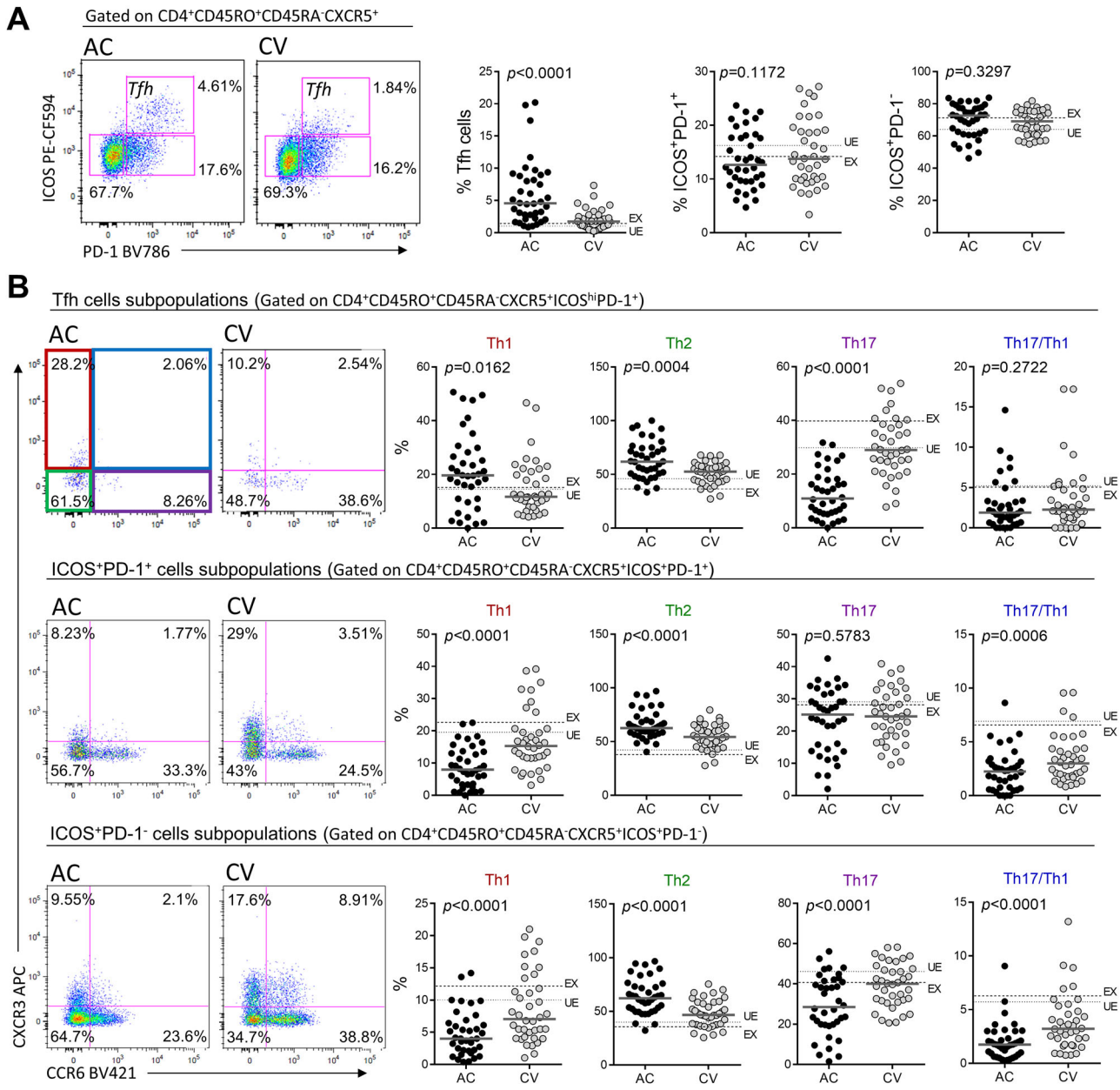

Figure 3. Expression of CXCR3 and CCR6 in circulating follicular helper T cells (cTfh) during *Plasmodium vivax* infection. PBMCs from *P. vivax*-infected adult patients ($n = 38$) were phenotyped by flow cytometry before (acute-phase sample, AC) and 28 days after starting curative chloroquine-primaquine treatment (convalescence sample, CV). Gating strategy is shown in Supporting information Fig. S7. (**A**) Representative density plots (left) and scatterplots (right) showing the frequency of cTfh ($ICOS^{hi}PD\text{-}1^{+}$) cells, $ICOS^{+}PD1^{+}$ cells, and $ICOS^{+}PD1^{-}$ cells within the $CD4^{+}CD45RA^{-}CD45RO^{+}CXCR5^{+}$ population. (**B**) Representative density plots (left) and scatterplots (right) showing the percentages of $CD4^{+}CD45RA^{-}CD45RO^{+}CXCR5^{+}ICOS^{hi}PD\text{-}1^{+}$ (cTfh cells) cells (upper panel), $CD4^{+}CD45RA^{-}CD45RO^{+}CXCR5^{+}ICOS^{+}PD1^{+}$ cells (middle panel), and $CD4^{+}CD45RA^{-}CD45RO^{+}CXCR5^{+}ICOS^{+}PD1^{-}$ cells (lower panel) with the Th1 ($CCR6^{-}CXCR3^{+}$), Th2 ($CCR6^{-}CXCR3^{-}$), double-positive of Th17/Th1 ($CCR6^{+}CXCR3^{+}$), and Th17 ($CCR6^{+}CXCR3^{-}$) phenotypes. Horizontal gray lines in scatterplots indicate median values for AC and CV patients. Horizontal dotted lines indicate median values for apparently healthy uninfected controls with similar age and sex distribution who were either malaria-exposed (EX; $n = 40$) or malaria-naïve (UE; $n = 20$). p Values for paired comparisons between AC and CV using the Wilcoxon signed rank test are indicated. See Supporting information Fig. S3 and Table S4 for comparisons between patient and control groups.

in the frequency of $CD19^{+}CD10^{+}$ immature B cells (Fig. 5A and Supporting information Fig. S4A; Supporting information Table S5). Significant changes during the infection were also found in the B-cell subsets defined by CD24 and CD38 expression levels [30], namely, a decreased frequency of $CD24^{hi}CD38^{lo}$ B cells and an increased frequency of $CD24^{lo}CD38^{lo}$ B cells (Fig. 5C and Supporting information Fig. S4C). The proportion of $CD24^{lo}CD38^{hi}$ cells was similar between AC and CV patients, and elevated in AC (but not CV) patients compared with EX control (Fig. 5C and Supporting information Fig. S4C; Supporting information Table S5).

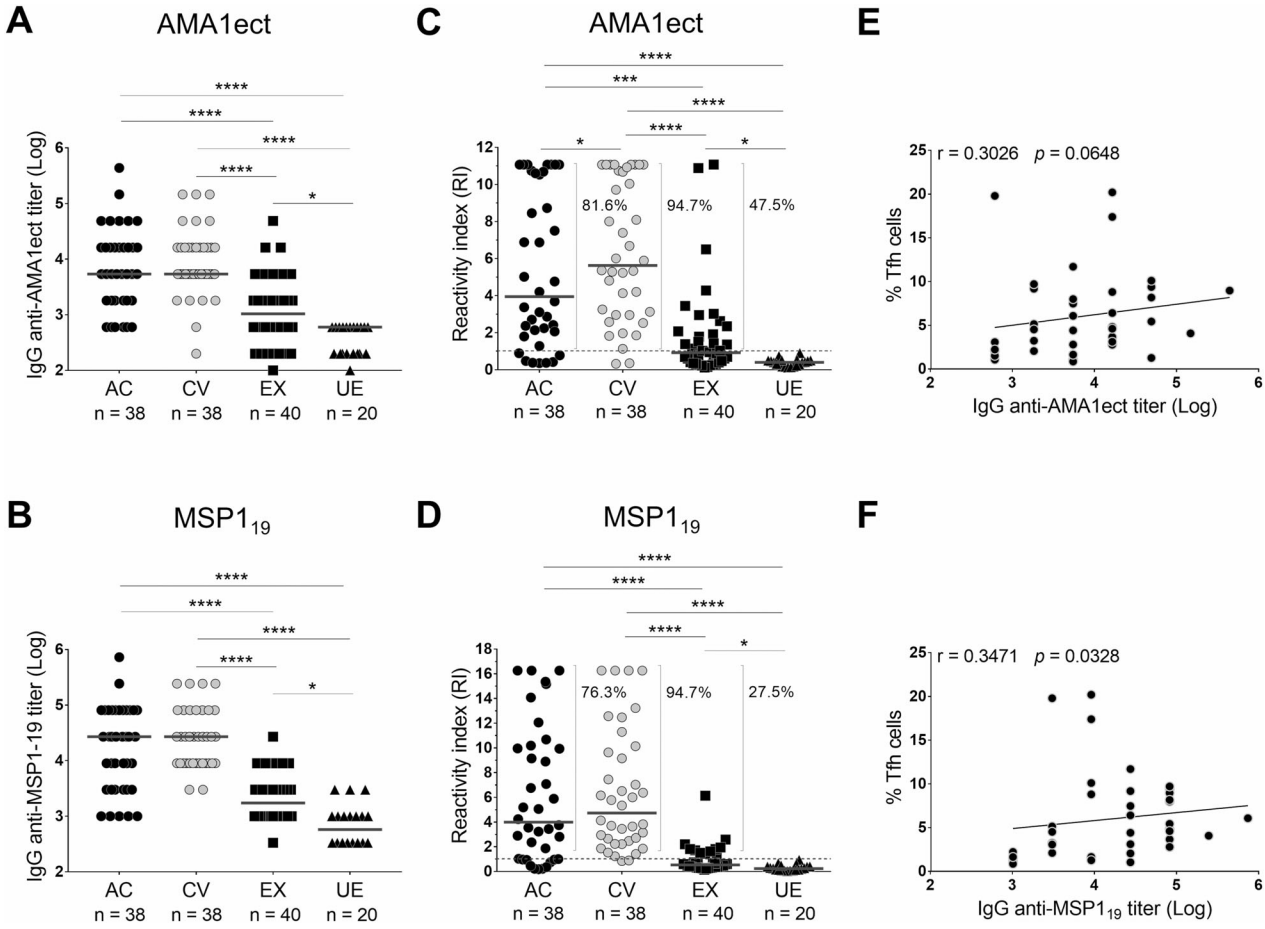

Figure 4. Antibody titers to the blood-stage antigens AMA1ect and MSP1$_{19}$ during *Plasmodium vivax* infection. Plasma samples from *P. vivax* infected adult patients ($n = 38$) were obtained before (AC) and 28 days after starting curative chloroquine-primaquine treatment (CV). Titers of anti-AMA1ect (**A**) and anti-MSP1$_{19}$ (**B**) IgG antibodies measured by ELISA were log-transformed for display. Reactivity indices of samples tested at 1:600 dilution (for AMA1ect) (**C**) and 1:3000 dilution (for MSP1$_{19}$) (**D**); positive samples have a reactivity index > 1. Horizontal gray lines in scatterplots indicate median values for AC, CV, EX, and UE patients; apparently healthy uninfected controls with similar age and sex distribution who were either malaria-exposed (EX; $n = 40$) or malaria-naïve (UE; $n = 20$). n = number of individuals analyzed in each group; percentages of antibody-positives are indicated. $^{*}p < 0.05$, $^{**}p < 0.01$, $^{***}p < 0.001$, $^{****}p < 0.0001$. AC and CV were compared by Wilcoxon test, and three groups (AC, EX and UE or CV, EX and UE) were compared by Kruskal–Wallis test with Dunn's multiple comparisons test. Spearman correlation between specific IgG titers to AMA1ect (**E**) and MSP1$_{19}$ (**F**) and the proportion (%) of cTfh cells.

Our data confirm the expansion of atypical memory B cells during acute malaria [27, 29], which persists after parasite clearance [29].

Circulating CD24^{hi}CD27^{+} Breg cells and IL-10 sources during *P. vivax* infection

IL-10 producing Breg cells are critical for modulating infection and reducing pathology in experimental murine malaria [31–33], but whether this applies to human malaria remains unclear [34]. We first examined the two major Breg cell subsets in the peripheral circulation of humans, namely, CD24^{hi}CD27^{+} B10-related cells and CD24^{hi}CD38^{hi} immature transitional cells [12]. There was a 25–40% reduction in the frequency of CD24^{hi}CD27^{+} Bregs in AC patients, compared to CV, EX, and UE individuals (Fig. 5D and Supporting information Fig. S4D; Supporting information Table S5), but no change in the CD24^{hi}CD38^{hi} Breg pool (Fig. 5C and Supporting information Fig. S4C; Supporting information Table S5). We next measured the proportion of B cells that produced IL-10 following ex vivo stimulation with lipopolysaccharide (LPS), phorbol 12-myristate 13-acetate (PMA), and ionomycin. Approximately 2% of circulating CD19^{+} B cells produced IL-10 when stimulated, with no significant differences when compared to the groups of participants (Fig. 6A and Supporting information Fig. S5A; Supporting information Table S6). However, the percentages of IL-10-producing CD24^{hi}CD27^{+} Breg cells, CD24^{hi}CD38^{hi} Breg cells, CD24^{hi}CD38^{lo} memory B cells, and CD24^{lo}CD38^{hi} plasma cells were significantly increased in AC patients compared to CV patients, and also to EX controls in most cases (Fig. 6A and Supporting information Fig. S5A; Supporting information Table S6). In contrast, the proportion of IL-10-producing CD24^{lo}CD38^{lo} B cells was approximately 10% lower in AC versus CV patients (Fig. 6A). We therefore show that *P. vivax*

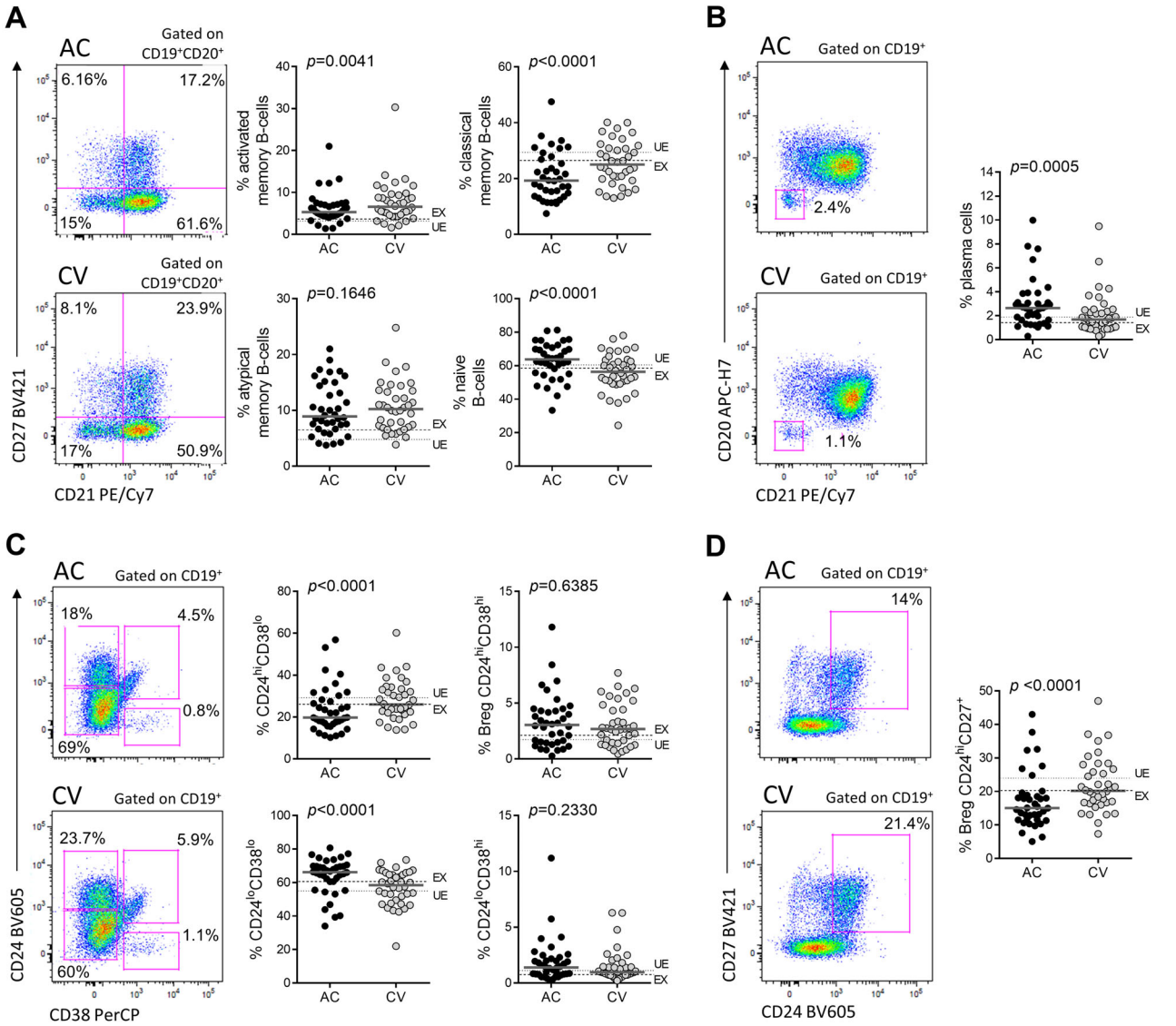

Figure 5. Characterization of B-cell compartment and circulating $CD24^{hi}CD27^{+}$ B regulatory cells in response to *Plasmodium vivax* infection. PBMCs from *P. vivax*-infected adult patients ($n = 38$) were phenotyped by flow cytometry before (acute-phase sample, AC) and 28 days after starting curative chloroquine-primaquine treatment (convalescence sample, CV). Gating strategy is shown in Supporting information Fig. S8. Representative density plots (left) and scatterplots (right) showing the percentages of $CD21^{-}CD27^{+}$ activated memory cells, $CD21^{+}CD27^{+}$ classic memory cells, $CD21^{-}CD27^{-}$ atypical memory cells, and $CD21^{+}CD27^{-}$ naïve cells within the $CD19^{+}CD20^{+}$ B-cell population (A) and circulating $CD20^{-}CD21^{-}$ plasma cells within the $CD19^{+}$ B-cell population (B). Representative density plots (left) and scatterplots (right) showing the percentages of $CD24^{hi}CD38^{lo}$, $CD24^{hi}CD38^{hi}$ regulatory B cells, $CD24^{lo}CD38^{lo}$, and $CD24^{lo}CD38^{hi}$ (C), and $CD24^{hi}CD27^{+}$ regulatory B cells, within the $CD19^{+}$ B-cell population (D). Horizontal gray lines in scatterplots indicate median values for AC and CV patients. Horizontal dotted lines indicate median values for apparently healthy uninfected controls with similar age and sex distribution who were either malaria-exposed (EX; $n = 40$) or malaria-naïve (UE; $n = 20$). *p* Values for paired comparisons between AC and CV using the Wilcoxon signed rank test are indicated. See Supporting information Fig. S4 and Supporting information Table S5 for comparisons between patient and control groups.

infection induced IL-10 production by B-cell subsets at levels comparable to those seen in malaria-naïve controls, and significantly higher than those in EX controls.

Decreased CD39 expression on Breg cells

During the acute infection, the expression of CD39—an ectonucleosidase involved in the generation of the anti-inflammatory molecule adenosine [35]—was found to be downregulated on both subsets of circulating $CD24^{hi}CD27^{+}$ Bregs (Fig. 6B and D) and $CD24^{hi}CD38^{hi}$ Bregs (Fig. 6C and E), compared to CV patients and also to controls in some cases (Supporting information Fig. S5B; Supporting information Table S7). Next, we focused on Bregs that are able to produce IL-10 upon unspecific stimulation. Across all groups of participants, the vast majority (>99%) of IL-10 producing $CD24^{hi}CD27^{+}$ Breg cells also expressed high levels of CD39 (Supporting information Table S8). Similar results

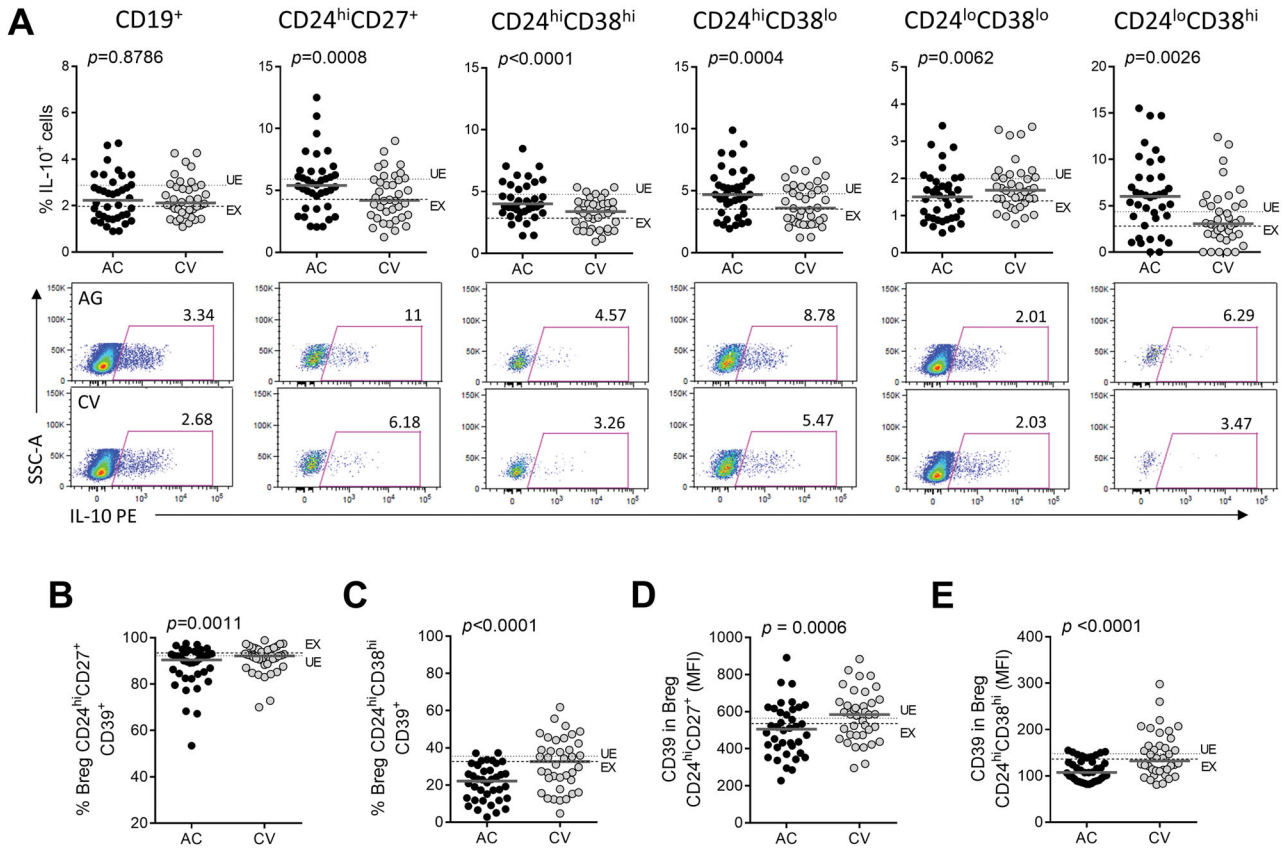

Figure 6. IL-10 production following unspecific B-cell stimulation ex vivo and expression of CD39 on $CD24^{hi}CD27^{+}$ and $CD24^{hi}CD38^{hi}$ Breg cells. PBMCs from *P. vivax* infected adult patients ($n = 38$) were analyzed before (acute-phase sample, AC) and 28 days after starting curative chloroquine-primaquine treatment (convalescence sample, CV). (A) Scatterplots (upper panel) and representative density plots (lower panel) showing the percentages of cells producing IL-10, upon ex vivo stimulation with LPS, PMA, and ionomycin, within the populations of $CD19^{+}$ B cells, $CD24^{hi}CD27^{+}$ Breg cells, $CD24^{hi}CD38^{hi}$ Breg cells, $CD24^{hi}CD38^{lo}$, $CD24^{lo}CD38^{lo}$, and $CD24^{lo}CD38^{hi}$ (from left to right). Gating strategy is shown in Supporting information Fig. S9. Scatterplots show the percentages of cells $CD24^{hi}CD27^{+}$ Breg cells and $CD24^{hi}CD38^{hi}$ Breg cells expressing CD39 (B and C) and the respective median fluorescence intensities (MFIs) for CD39 (D and E). The overall gating strategy is shown in Supporting information Fig. S8. Horizontal gray lines in scatterplots indicate median values for AC and CV patients. Horizontal dotted lines indicate median values for apparently healthy uninfected controls with similar age and sex distribution who were either malaria-exposed (EX; $n = 40$) or malaria-naïve (UE; $n = 20$). p Values for paired comparisons between AC and CV using the Wilcoxon signed rank test are indicated. See Supporting information Fig. S5 and Tables S6 and S7 for comparisons between patient and control groups.

were found for the overall population of IL-10-producing $CD19^{+}$ B cells, $CD24^{hi}CD38^{lo}$, $CD24^{lo}CD38^{lo}$, and $CD24^{lo}CD38^{hi}$ cells, consistent with an extensive overlap between IL-10-producing and $CD39^{hi}$ B-cell subsets. These results suggest that CD39 is specifically upregulated in the Breg cells subsets that produce IL-10, regardless of the infection status of the donors, consistent with a regulatory phenotype for $CD39^{hi}$ B cells [36]. There was, however, an exception: fewer IL-10-producing $CD24^{hi}CD38^{hi}$ immature transitional Breg cells were $CD39^{hi}$ in AC patients (median, 37%), compared to median proportions of 48% $CD39^{hi}$ cells in CV patients ($p = 0.0044$) and 50–51% in EX and UE controls ($p = 0.0002$) (Supporting information Table S8).

Discussion

Here, we characterize how $CD4^{+}$ T- and B-cell populations respond to *P. vivax* infection in patients continuously exposed to relatively high malaria transmission in the Amazon. Table 1 summarizes the extensive changes seen in the frequencies of peripheral-blood cell subsets during the infection. In this table, to identify a difference between currently (AC) or recently (CV) infected individuals and controls, we considered primarily local, EX control subjects. Therefore, differences between CV and EX, even if not confirmed when comparing CV and UE, were considered as indicative of changes that persist after infection. In the cases where changes did not show statistical difference between groups that sustain the result, we added a question mark.

We first examined two T regulatory cell subsets. Consistent with previous observations [15, 24, 25], we found an increased frequency of CD4 Treg cells that express CTLA-4 circulating during the acute infection, which are key contributors to Th cell downregulation in malaria patients [3, 25]. Importantly, CTLA-4 expression levels correlated positively with parasite density measured by quantitative PCR, consistent with a

Table 1. Main changes observed in the frequency of circulating CD4 T regulatory (Treg) cells, T follicular regulatory (Tfr) cells, T follicular helper (cTfh), and B cells during *Plasmodium vivax* infection.

Cell population	Phenotype	Change
CTLA-4-expressing CD4 Treg	$CD4^+CD45RA^-CD25^+FoxP3^+CTLA\text{-}4^+$	Transient increase
CTLA-4-expressing Tfr	$CD4^+CD45RA^-CD25^+FoxP3^+\ CXCR5^+CTLA\text{-}4^+$	Transient increase
CD4 T memory cells	$CD4^+CD45RO^+CD45RA^-$	Increase during convalescence?[a]
Th1 CD4 T memory cells	$CD4^+CD45RO^+CD45RA^-CCR6^-CXCR3^+$	Sustained decrease
Th2 CD4 T memory cells	$CD4^+CD45RO^+CD45RA^-CCR6^-CXCR3^-$	Sustained increase
Th17 CD4 T memory cells	$CD4^+CD45RO^+CD45RA^-CCR6^+CXCR3^-$	Transient decrease
Th17/Th1 CD4 memory cells	$CD4^+CD45RO^+CD45RA^-CCR6^+CXCR3^+$	Sustained decrease
Th1 cTfh cells	$CD4^+CD45RA^-CD45RO^+CXCR5^+$ $ICOS^{hi}PD\text{-}1^+CCR6^-CXCR3^+$	Transient increase
Th2 cTfh cells	$CD4^+CD45RA^-CD45RO^+CXCR5^+$ $ICOS^{hi}PD\text{-}1^+CCR6^-CXCR3^-$	Sustained increase
Th17 cTfh cells	$CD4^+CD45RA^-CD45RO^+CXCR5^+\ ICOS^{hi}PD\text{-}1^+$ $CCR6^+CXCR3^-$	Sustained decrease
Th17/Th1 cTfh cells	$CD4^+CD45RA^-CD45RO^+CXCR5^+\ ICOS^{hi}PD\text{-}1^+$ $CCR6^+CXCR3^+$	Sustained decrease
B cells	$CD19^+$	Transient increase
Immature B cells	$CD19^+CD10^+$	No significant change
Plasma cells	$CD19^+CD20^-CD21^-$	Transient increase
Activated memory B cells	$CD19^+CD20^+CD21^-CD27^+$	Sustained increase
Classical memory B cells	$CD19^+CD20^+CD21^+CD27^+$	Transient decrease
Naïve B cells	$CD19^+CD20^+CD21^+CD27^-$	Transient increase
Atypical memory B cells	$CD19^+CD20^+CD21^-CD27^-$	Sustained increase
Memory B cells	$CD19^+CD24^{hi}CD38^{lo}$	Transient decrease
Naïve mature B cells	$CD19^+CD24^{lo}CD38^{lo}$	Transient increase
Plasma cells/plasmablasts	$CD19^+CD24^{lo}CD38^{hi}$	Transient increase?[b]
Immature transitional Breg cells	$CD19^+CD24^{hi}CD38^{hi}$	No significant change
B10-related Breg cells	$CD19^+CD24^{hi}CD27^+$	Transient decrease

[a] CV > AC, but no statistically significant difference was found between CV and EX, and between CV and UE.
[b] AC > EX, but AC = CV, and CV = EX and UE.

dose–response effect. Due to the limited number of cells available for immunophenotyping, we were unable to characterize the expression of other surface inhibitory molecules (e.g., lymphocyte activation gene-3 [LAG-3], programmed death-1 [PD-1], and T-cell immunoglobulin mucin-3 [TIM-3]) on Tregs. In addition, we identified for the first time in vivax malaria patients an expansion of a distinct subset of circulating Treg cells, namely, $CD4^+CD45RA^-CD25^+FoxP3^+CXCR5^+$ Tfr cells expressing CTLA-4 [37], which correlated positively with parasite density. The primary physiological role of Tfr cells is to limit the development of autoreactive B cells and, together with Tfh cells, control germinal center responses [38]. Increased frequencies of $CTLA\text{-}4^+$ Tfr cells were also recently described in *P. falciparum* infected febrile African children [3]. Importantly, CTLA-4 deletion results in compromised effector function of Tfr cells in mice [39, 40], consistent with the key role of this primary inhibitory receptor. Circulating Tfr cells are thought to display an incomplete suppressive function, compared to those within lymphoid tissues, probably because they leave these tissues while still immature [41]. We suggest that the relative proportion of Tfr versus Tfh cells and the expression levels of CTLA-4 on Tfr cells are key parameters to understand the Tfh–B cell cooperation in human malaria. However, their role in malaria immunity still remains unknown and requires further studies.

We describe a Th2 bias in circulating memory $CD4^+$ T cells, but an expansion of both Th1 and Th2 subpopulations only in $CXCR5^+ICOS^{hi}PD\text{-}1^+$ cTfh cells within the memory $CD4^+$ T cell pool of vivax malaria patients. It is important to emphasize that other populations of $CD4^+$ T cells expressing CXCR5 ($ICOS^+PD\text{-}1^+$ and $ICOS^+PD\text{-}1^-$), observed in our study, did not show expansion of Th1 cells during *P. vivax* infection; this means that considering Tfh cells only by the expression of CXCR5 can change the results when populations of some cells are evaluated. Not surprisingly, the cTfh cell expansion during acute infection correlated positively with the titers of anti-$MSP1_{19}$ antibodies (this study) and the cumulative exposure to malaria [27]. However, the Th1 polarization of cTfh cell responses described in *P. falciparum* infected African children [9] and *P. vivax* infected Amazonian adults [27] was not confirmed in the present study. Moreover, cTfh cell frequencies did not correlate with the titer or breadth of specific malaria antibody response in African children [9]. Importantly, Th1-biased cTfh cells are often seen as a hallmark

of poor naturally acquired antibody responses in human malaria [13]. For example, Th1-restricted cTfh responses are linked to the development of atypical memory B cells in children with *P. falciparum* malaria [42], which also occur in increased frequencies in *P. vivax* infection ([27, 29]; this study).

Factors such as age, malaria exposure, and the duration of infection can differentially modulate the expansion of Th1-, Th2-, and Th17-type cTfh cells in response to *P. falciparum* infection [7, 43, 44]. First, an early Th2 bias in the cTfh pool is seen at peak parasitemia in experimental human challenge with *P. falciparum*, followed by a markedly increased proportion of Th1 cTfh cells one week after treatment [7]. Moreover, ex vivo stimulation of PBMCs from malaria-naïve donors with *P. falciparum* infected red blood cells recapitulates the activation of both Th1 and Th2 subsets of cTfh cells [7]. These findings suggest that individual and contextual factors are likely to modulate the Th1/Th2 balance of cTfh cells over the course of human malaria, with clear implications for antibody-mediated protection triggered by natural infection or vaccines. However, understanding how antigen-specific Tfh cells differentiate and function in human malaria remains an elusive goal, as these cells do not circulate in the peripheral blood and secrete small quantities of cytokines [38].

Breg cells are key regulators of inflammation and pathology in experimental murine malaria [31–33]. Here, we provide the first characterization of circulating Breg cells in human malaria, showing a decreased frequency of B10-related Breg cells ($CD24^{hi}CD27^{+}$) and no significant change in the $CD19^{+}CD24^{hi}CD38^{hi}$ Breg population. These Breg cell phenotypes may play different immunoregulatory roles [12]. $CD24^{hi}CD27^{+}$ Breg cells are able to suppress effector $CD4^{+}$ T cells [45], while $CD24^{hi}CD38^{hi}$ Breg cells were shown to be able to convert $CD4^{+}CD25^{-}$ T cells into Treg cells [46]. Breg cells are thought to promote the differentiation of Tfr and Treg cells with suppressive capacity (since they express CTLA4) in the secondary lymphoid organs. Moreover, after ex vivo stimulation we found only a modest increase in IL-10 production by $CD19^{+}CD24^{hi}CD27^{+}$ and $CD19^{+}CD24^{hi}CD38^{hi}$ cells circulating during acute *P. vivax* infection. We therefore suggest that peripheral blood Breg cell subsets are unlikely to be a major source of IL-10, but Bregs can still play a key role in regulating T-cell driven immune responses in vivax malaria in secondary lymphoid organs.

There are important limitations inherent to our findings. First, we characterized $CD4^{+}$ T- and B-cell populations limited to the circulating pool, as we had no access to secondary lymphoid tissues from malaria patients. Moreover, these cells were cryopreserved before immunophenotyping, and we cannot rule out the risk of selectively losing some cell subpopulations during the freeze/thaw cycle. Second, we obtained PBMC samples at only two timepoints, during and shortly after *P. vivax* infection; no baseline cell frequency data were available for the same participants, before infection, to causally link infection with cell population changes. We therefore have characterized statistical associations, rather than causal relationships between infection and cellular responses. Third, there are limitations pertinent to the study population. We enrolled patients from the main malaria hotspot in Brazil (annual parasite incidence [API] > 500 cases per 1000 inhabitants), whose responses to *P. vivax* infection may not be directly comparable to populations exposed to substantially lower transmission, such as those studied by Figueiredo et al. [27] (API estimated at 50 cases per 1000 inhabitants). In addition, our study participants are not exclusively exposed to *P. vivax*, as low-level transmission of *P. falciparum* persists in the area. This species accounts for 14% of the local malaria burden [26]. Moreover, as all study participants were adults with overt clinical manifestations of *P. vivax* malaria at baseline, we did not have a comparison group consisting of "clinically immune" individuals, who may remain symptomless despite being infected. Fourth, differences in the way cTfh and B cells have been phenotypically defined may undermine comparisons between studies. For instance, here we use a strict definition of cTfh cells ($CD4^{+}CD45RA^{-}CD45RO^{+}CXCR5^{+}ICOS^{hi}PD\text{-}1^{+}$) that have not been previously applied to malaria-exposed populations. In addition, we analyzed B-cell populations by considering CD21 and CD27 expression levels within the population of $CD19^{+}CD20^{+}$ cells. This gating strategy is not widely used but allows to exclude plasma cells ($CD20^{-}CD21^{-}$) that might confound the analysis of atypical memory B cells ($CD21^{-}CD27^{-}$) and memory activated cells ($CD21^{-}CD27^{+}$).

In conclusion, we describe how a range of peripheral-blood $CD4^{+}$ T- and B-cell subsets with effector and regulatory roles respond to *P. vivax* infection. We identify changes associated with human malaria in understudied cell populations, such as the increased frequency of CTLA-4^{+} Tfr cells and the reduced frequency of B10-related Breg cells in acute-phase patients. Importantly, we challenge the notion that cTfh responses are Th1-polarized in human malaria [13, 27] and identify an expansion of both Th1 and Th2 cTfh cells in *P. vivax*-infected adults. Overall, the complex immunoregulatory network triggered by *P. vivax* infection in adults continuously exposed to malaria transmission, but still susceptible to clinical malaria, comprises a wide range of cell subsets—some of which characterized for the first time in the peripheral blood of vivax malaria patients, such as CTLA-4^{+} Tfr cells and Breg cells—that may be specifically targeted by improved vaccination strategies in the near future.

Materials and methods

Study site and population

Participants were enrolled in August–September 2017 in the town of Mâncio Lima (population: 8800), upper Juruá Valley, next to the border with Peru. The local API was estimated at 521 malaria cases per 1000 inhabitants in 2017, the highest for a municipality in Brazil (Ministry of Health of Brazil, 2018). Mâncio Lima receives most rainfall between November and April, but malaria transmission occurs year-round. *Plasmodium vivax* accounted for 84.2% of local malaria cases and *P. falciparum* for 14.4%; 1.4%

were coinfections with both species [26]. The primary malaria vector is *An. darlingi*, which thrives in natural breeding sites and fish farming tanks [47].

We obtained PBMCs to characterize circulating T- and B-cell subsets, plasma to measure antibodies, and DNA for molecular diagnosis of malaria. To this end, we collected 76 mL pretreatment, acute-phase (AC) venous blood samples from 38 participants with single-species uncomplicated *P. vivax* infection (age range, 18–70 years). On-site microscopic diagnosis of malaria was confirmed by species-specific quantitative real-time PCR that targets the *18SrRNA* gene of *P. falciparum* and *P. vivax*, with a detection threshold between 1.5 and 2 parasites/μL, respectively, of blood. Standard curves were prepared with serial 10-fold dilutions of the target sequences, cloned into pGEM-T Easy vectors (Promega, Madison, WI), to allow for quantitation of parasite loads as number of parasites per milliliter of blood [15].

In addition, we collected a paired convalescence (CV) blood sample around 28 days (range, 26–30 days) after the start of chloroquine (25 mg/kg of body weight over 3 days)–primaquine (3.5 mg/kg over 7 days) treatment. This therapy was highly efficacious in the study site at the time of the study [48]. We also collected blood samples from 40 apparently healthy subjects living in the same area, who reported no laboratory-confirmed malaria attack within the past 6 months and were negative for malaria parasites, and thus served as malaria-exposed (EX) but noninfected controls (age range, 18–68 years). Finally, we collected blood samples from 20 apparently healthy subjects living in malaria-free São Paulo city, in Southeast Brazil, who served as malaria-unexposed (UE) controls (age range, 19–56 years; Supporting information Table S1). None of the female participants was pregnant. CV, EX, and UE participants were negative for malaria parasites by quantitative real-time PCR. Full blood cell counts and hemoglobin measurements were performed using an ABX Micros 60 automated cell counter (Horiba, Montpellier, France) (Supporting information Table S1). Plasmas for antibody measurements were obtained by centrifugation of heparinized blood samples, shipped to São Paulo on dry ice, and stored at −20°C until tested for antibodies.

Peripheral-blood mononuclear cells

PBMCs were separated by gradient centrifugation with Ficoll-Paque Plus (GE Healthcare, United Kingdom), within 10 h of blood collection, and cryopreserved in liquid nitrogen as described [15]. PBMCs were thawed at 37°C in a water bath, washed in R10 medium (Gibco, Scotland), and resuspended in RPMI 1640 medium (Gibco) supplemented with 10% (vol/vol) inactivated fetal bovine serum (HyClone, Cytiva), 10 mM HEPES (Gibco), 2 mM L-glutamine (Gibco), 1 mM sodium pyruvate (Gibco), 55 mM 2-mercaptoethanol (Gibco), and a 1% (vol/vol) solution containing 100 U/mL of penicillin, 10 mg/mL of streptomycin, and 25 mg/mL of amphotericin B (Gibco). PBMCs were evaluated for viability using Trypan Blue (Sigma-Aldrich) with cell counts in Neubauer chamber; only samples with >80% viability were used for flow cytometry analysis.

Monoclonal antibody panels

Four different antibody panels were used to characterize Tregs and Tfr cells (panel 1; Supporting information Table S9; gating strategy in Supporting information Fig. S6), Tfh cell subsets (panel 2; Supporting information Table S10; gating strategy in Supporting information Fig. S7), B-cell subsets (panel 3; Supporting information Table S11; gating strategy in Supporting information Fig. S8), and IL-10-producing B cells (panel 4; Supporting information Table S12; gating strategy in Supporting information Fig. S9). We titrated each antibody and selected its final dilution for an optimal specific staining associated with a low background.

CD4 T- and B-cell phenotyping by flow cytometry

Thawed PBMC samples were centrifuged at 500 *g* for 8 min, and 1.5×10^6 viable cells per well were suspended in 50 μL of staining buffer (PBS with 2% fetal bovine serum) in V-bottomed 96-well microplates (Thermo-Fisher, USA) and incubated with Fc-receptor blocking antibodies (Fc Block, BD Biosciences) for 10 min at room temperature. Following staining with viability dye (Live/Dead Aqua, Invitrogen), cell surface staining was carried out with the specific antibodies listed in each panel. Cells were incubated at room temperature in darkness for 20 min, washed twice with staining buffer, and fixed with 1% paraformaldehyde. For FoxP3 expression analysis (see Supporting information Table S9 for antibodies), cells were fixed and permeabilized using the FOXP3 Fix/Perm Buffer (BioLegend) kit, stained with anti-FoxP3 antibodies diluted in FOXP3 Perm buffer (BioLegend) for 40 min, washed, and resuspended in staining buffer. Samples were acquired on an LSR Fortessa flow cytometer (BD Biosciences) using the FACSDiva software (BD Biosciences), and a total of 10^6 events were collected in each sample. Anti-mouse (BD CompBead Anti-Mouse Ig, BD Biosciences) and anti-rat/hamster IgG-coated beads (BD CompBead Anti-Rat/Anti-Hamster Ig, BD Biosciences) were stained with each fluorochrome separately and used for voltage adjustment and software-based compensation, in addition to beads (ArC Amine Reactive Compensation Bead kit, Invitrogen) labeled with viability dye (Live/Dead Aqua, Invitrogen). Data analysis was carried out using FlowJo software version 9.9 (Tree Star, USA). Gating strategies are presented in Supporting information Figs. S6 (Tregs and Tfr cells), S7 (Tfh cells), and S8 (B-cell subsets). Fluorescence minus one controls were used in all panels, for Tregs and Tfr cells (Supporting information Fig. S10A), Tfh cells (Supporting information Fig. S10B), and B-cell subsets (Supporting information Fig. S11A) in order to control for spectral overlap and gate positions. All experiments involving flow cytometry were executed according to the MIATA guidelines.

Antibody measurements

We used blood-stage *P. vivax* antigens expressed as recombinant proteins to capture IgG antibodies: (a) residues 43–487 of the *P. vivax* apical membrane antigen 1 ectodomain (AMA1ect), expressed in *Pichia pastoris* [49] and (b) the C-terminal, 19 kDa region of *P. vivax* merozoite surface protein 1 ($MSP1_{19}$), Belém strain, expressed in *Escherichia coli* [50]. Methods for protein expression and purification have been described elsewhere [49, 50]. Enzyme immunoassay (ELISA) was used to measure antigen-specific IgG antibodies. Briefly, high-binding 96-well Costar microplates (Corning, Corning, NY) were coated with 100 ng/well of solid-phase antigen in phosphate-buffered saline for 16 h at room temperature. Duplicate plasma samples were serially diluted (eight dilutions, factor 3) starting at 1:200 (followed by 1:600, 1:1800, etc.) for AMA1ect, and 1:1000 (followed by 1:3000, 1:9000, etc.) for $MSP1_{19}$, with 100 μL/well of each dilution being incubate for 2 h at room temperature. Antibody binding to solid-phase antigen was detected with peroxidase-conjugated goat anti-human IgG (Jackson ImmunoResearch, St. Thomas' Place, UK). After the use of o-phenylenediamine and hydrogen peroxide at acidic pH as a substrate, absorbance values were measured at 490 nm. Reactivity indices were calculated as the ratio between the absorbance values of each test sample, at 1:600 for AMA1ect and 1:3000 for $MSP1_{19}$, and the antigen-specific cut-off value, corresponding to the average absorbance for plasmas from 20 malaria-naïve donors plus 3 standard deviations. Positive samples were those with reactivity indice > 1. The calculate antibody titers were defined as the greatest plasma dilution giving an absorbance value above 0.1. Titers were log transformed for display on figures.

Measurement of IL-10 production upon stimulation of B-cell subsets

We used intracellular cytokine staining to identify the production and accumulation of IL-10, upon stimulation with LPS followed by PMA and ionomycin, within the endoplasmic reticulum of $CD19^+$ cells. To this end, 1.5×10^6 PBMCs/well were cultured in duplicate in U-bottomed 96-well microplates at 37°C for 19 h in the absence (medium alone) or presence of LPS (1 μg/mL). LPS-stimulated cells were further incubated with 50 ng/mL of PMA (Sigma-Aldrich) and 1 μg/mL of ionomycin, while nonstimulated cells were maintained in medium alone. PBMCs were treated with brefeldin A (BD GolgiPlug) and monensin (BD GolgiStop), to retain cytokines within the cell, and kept for 5 h at 37°C in a CO_2 incubator (total incubation, 24 h). Next, the duplicates were merged and PBMCs were transferred to V-bottomed 96-well microplates for cell surface and IL-10 intracellular staining with the monoclonal antibodies listed in Supporting information Table S12. Gating strategies are presented in Supporting information Fig. S9 with the Fluorescence minus one controls shown in Supporting information Fig. S11B.

Statistical analysis

Because most continuous variables were not normally distributed, results were summarized as medians and interquartile ranges. The D'Agostino-Pearson normality test was performed only on demographic and blood cell count data. Nonparametric tests were applied to ELISA and flow cytometry results. Comparisons across AC, EX, and UE or CV, EX, and UE participants were done with nonparametric Kruskal–Wallis (for continuous variables not normally distributed), parametric ANOVA (for normally distributed continuous variables), or χ^2 tests (for proportions). When individual Kruskal–Wallis tests or ANOVA indicated a significant difference among groups ($p < 0.05$, two-sided tests), Dunn's or Tukey's multiple comparison tests were carried out to determine where the differences lay. Significant differences between AC versus EX and UE were assumed to indicate changes associated with acute infection. To compare results from two independent participant groups (AC vs. EX), we used the Mann–Whitney test. Paired data (AC vs. CV) were compared with the paired *t* test or Wilcoxon signed rank test for continuous variables, or McNemar tests for proportions to test whether significant changes observed during acute infection were sustained (i.e., AC = CV) or transient (i.e., AC ≠ CV). Nonparametric correlation coefficients (r_s) were estimated using Spearman rank correlation tests. All analyses were performed using GraphPad Prism 7.04 (GraphPad, San Diego, CA).

Acknowledgements: We thank all blood donors for their participation in the study; Odailton A. Nery, Elbem S. Rocha, Mario S. Mendes, Maria de Fátima Melo, Maria Urlaete A. Silva, Marísia S. do Vale, Vera L. Carvalho, Francisco M. Santos, and Rodrigo M. de Souza (Federal University of Acre, Brazil) for logistic support during field work; and Márcio M. Yamamoto, Priscila T. Rodrigues, and Lais C. Salla for laboratory support. This work was supported by the Fundação de Amparo à Pesquisa do Estado de São Paulo (FAPESP), Brazil (2016/50108-0 to ISS, 2016/18740-9 to MUF, and 2018/07142-9 to SBB), the Coordenação de Aperfeiçoamento de Pessoal de Nível Superior (CAPES) (Finance code 001), and the National Institutes of Health, as part of the International Centers of Excellence in Malaria Research program (U19 AI089681 subcontract to MUF). NSF was supported by doctoral scholarships from CAPES and the Conselho Nacional de Desenvolvimento Científico e Tecnológico (CNPq); ISS, MUF, and SBB receive senior research scholarships from CNPq; and MUF received a visiting scholarship from the Casa da América Latina and Fundação Millennium BCP.

Conflict of interest: The authors declare no commercial or financial conflict of interest.

Author contributions: N.S.F., M.U.F., and S.B.B. designed the study. N.S.F. and N.F.L. conducted field sample collection. N.S.F performed the experiments. I.S.S., M.U.F., and S.B.B. provided key reagents. N.S.F. and F.B.S. performed the cytometry analysis. N.S.F. performed the statistical and data analysis. N.S.F., M.U.F., and S.B.B. wrote the manuscript. M.U.F. and S.B.B. supervised the study.

Ethics approval: The study protocol was approved by the institutional review board of the Institute of Biomedical Sciences, University of São Paulo (CAAE # 56893016.5.0000.5467, protocol #1347/16). All participants were >18 years old and provided written informed consent prior to participation.

Data availability statement: The data that support the findings of this study are available from the corresponding authors upon reasonable request.

Peer review: The peer review history for this article is available at https://publons.com/publon/10.1002/eji.202350372

References

1 **Battle, K. E., Lucas, T. C. D., Nguyen, M., Howes, R. E., Nandi, A. K., Twohig, K. A., Pfeffer, D. A., et al.**, Mapping the global endemicity and clinical burden of *Plasmodium vivax*, 2000–17: a spatial and temporal modelling study. *Lancet* 2019. **394**: 332–343.

2 **Weiss, D. J., Lucas, T. C. D., Nguyen, M., Nandi, A. K., Bisanzio, D., Battle, K. E., Cameron, E., et al.**, Mapping the global prevalence, incidence, and mortality of *Plasmodium falciparum*, 2000–17: a spatial and temporal modelling study. *Lancet* 2019. **394**: 322–331.

3 **Kurup, S. P., Obeng-Adjei, N., Anthony, S. M., Traore, B., Doumbo, O. K., Butler, N. S., Crompton, P. D., et al.**, Regulatory T cells impede acute and long-term immunity to blood-stage malaria through CTLA-4. *Nat. Med.* 2017. **23**: 1220–1225.

4 **Gbedande, K., Carpio, V. H. and Stephens, R.**, Using two phases of the CD4 T cell response to blood-stage murine malaria to understand regulation of systemic immunity and placental pathology in *Plasmodium falciparum* infection. *Immunol. Rev.* 2020. **293**: 88–114.

5 **Locci, M., Havenar-Daughton, C., Landais, E., Wu, J., Kroenke, M. A., Arlehamn, C. L., Su, L. F., et al.**, Human circulating PD-1+CXCR3-CXCR5+ memory Tfh cells are highly functional and correlate with broadly neutralizing HIV antibody responses. *Immunity* 2013. **39**: 758–769.

6 **Reinhardt, R. L., Liang, H. E. and Locksley, R. M.**, Cytokine-secreting follicular T cells shape the antibody repertoire. *Nat. Immunol.* 2009. **10**: 385–393.

7 **Chan, J. A., Loughland, J. R., de Labastida Rivera, F., SheelaNair, A., Andrew, D. W., Dooley, N. L., Wines, B. D., et al.**, Th2-like T follicular helper cells promote functional antibody production during *Plasmodium falciparum* infection. *Cell Rep. Med.* 2020. **1**: 100157.

8 **Morita, R., Schmitt, N., Bentebibel, S. E., Ranganathan, R., Bourdery, L., Zurawski, G., Foucat, E., et al.**, Human blood CXCR5(+)CD4(+) T cells are counterparts of T follicular cells and contain specific subsets that differentially support antibody secretion. *Immunity* 2011. **34**: 108–121.

9 **Obeng-Adjei, N., Portugal, S., Tran, T. M., Yazew, T. B., Skinner, J., Li, S., Jain, A., et al.**, Circulating Th1-cell-type Tfh cells that exhibit impaired B cell help are preferentially activated during acute malaria in children. *Cell Rep.* 2015. **13**: 425–439.

10 **Hviid, L., Barfod, L. and Fowkes, F. J.**, Trying to remember: immunological B cell memory to malaria. *Trends Parasitol.* 2015. **31**: 89–94.

11 **Sage, P. T. and Sharpe, A. H.**, The multifaceted functions of follicular regulatory T cells. *Curr. Opin. Immunol.* 2020. **67**: 68–74.

12 **Hasan, M. M., Thompson-Snipes, L., Klintmalm, G., Demetris, A. J., O'Leary, J., Oh, S. and Joo, H.**, CD24(hi)CD38(hi) and CD24(hi)CD27(+) human regulatory B cells display common and distinct functional characteristics. *J. Immunol.* 2019. **203**: 2110–2120.

13 **Yap, X. Z., Hustin, L. S. P. and Sauerwein, R. W.**, TH1-polarized TFH cells delay naturally-acquired immunity to malaria. *Front. Immunol.* 2019. **10**: 1096.

14 **Antonelli, L. R., Junqueira, C., Vinetz, J. M., Golenbock, D. T., Ferreira, M. U. and Gazzinelli, R. T.**, The immunology of *Plasmodium vivax* malaria. *Immunol. Rev.* 2020. **293**: 163–189.

15 **Goncalves, R. M., Salmazi, K. C., Santos, B. A., Bastos, M. S., Rocha, S. C., Boscardin, S. B., Silber, A. M., et al.**, CD4+ CD25+ Foxp3+ regulatory T cells, dendritic cells, and circulating cytokines in uncomplicated malaria: do different parasite species elicit similar host responses? *Infect. Immun.* 2010. **78**: 4763–4772.

16 **Kanjee, U., Rangel, G. W., Clark, M. A. and Duraisingh, M. T.**, Molecular and cellular interactions defining the tropism of *Plasmodium vivax* for reticulocytes. *Curr. Opin. Microbiol.* 2018. **46**: 109–115.

17 **Wahlgren, M., Goel, S. and Akhouri, R. R.**, Variant surface antigens of *Plasmodium falciparum* and their roles in severe malaria. *Nat. Rev. Microbiol.* 2017. **15**: 479–491.

18 **Carvalho, B. O., Lopes, S. C., Nogueira, P. A., Orlandi, P. P., Bargieri, D. Y., Blanco, Y. C., Mamoni, R., et al.**, On the cytoadhesion of *Plasmodium vivax*-infected erythrocytes. *J. Infect. Dis.* 2010. **202**: 638–647.

19 **Lopes, S. C., Albrecht, L., Carvalho, B. O., Siqueira, A. M., Thomson-Luque, R., Nogueira, P. A., Fernandez-Becerra, C., et al.**, Paucity of *Plasmodium vivax* mature schizonts in peripheral blood is associated with their increased cytoadhesive potential. *J. Infect. Dis.* 2014. **209**: 1403–1407.

20 **White, N. J. and Imwong, M.**, Relapse. *Adv. Parasitol.* 2012. **80**: 113–150.

21 **Longley, R. J., Sattabongkot, J. and Mueller, I.**, Insights into the naturally acquired immune response to *Plasmodium vivax* malaria. *Parasitology* 2016. **143**: 154–170.

22 **Mueller, I., Galinski, M. R., Tsuboi, T., Arevalo-Herrera, M., Collins, W. E. and King, C. L.**, Natural acquisition of immunity to *Plasmodium vivax*: epidemiological observations and potential targets. *Adv. Parasitol.* 2013. **81**: 77–131.

23 **McKenzie, F. E., Prudhomme, W. A., Magill, A. J., Forney, J. R., Permpanich, B., Lucas, C., Gasser, R. A. Jr., et al.**, White blood cell counts and malaria. *J. Infect. Dis.* 2005. **192**: 323–330.

24 **Bueno, L. L., Morais, C. G., Araujo, F. F., Gomes, J. A., Correa-Oliveira, R., Soares, I. S., Lacerda, M. V., et al.**, *Plasmodium vivax*: induction of CD4+CD25+FoxP3+ regulatory T cells during infection are directly associated with level of circulating parasites. *PLoS One* 2010. **5**: e9623.

25 **Costa, P. A., Leoratti, F. M., Figueiredo, M. M., Tada, M. S., Pereira, D. B., Junqueira, C., Soares, I. S., et al.**, Induction of inhibitory receptors on T cells during *Plasmodium vivax* malaria impairs cytokine production. *J. Infect. Dis.* 2015. **212**: 1999–2010.

26 **Corder, R. M., Paula, G. A., Pincelli, A. and Ferreira, M. U.**, Statistical modeling of surveillance data to identify correlates of urban malaria risk: a population-based study in the Amazon Basin. *PLoS One* 2019. **14**: e0220980.

27 **Figueiredo, M. M., Costa, P. A. C., Diniz, S. Q., Henriques, P. M., Kano, F. S., Tada, M. S., Pereira, D. B., et al.**, T follicular helper cells regulate the

activation of B lymphocytes and antibody production during *Plasmodium vivax* infection. *PLoS Pathog.* 2017. **13**: e1006484.

28 **Patgaonkar, M., Herbert, F., Powale, K., Gandhe, P., Gogtay, N., Thatte, U., Pied, S., et al.**, Vivax infection alters peripheral B-cell profile and induces persistent serum IgM. *Parasite Immunol.* 2018. **40**: e12580.

29 **Soares, R. R., Cunha, C. F., Ferraz-Nogueira, R., Marins-Dos-Santos, A., Rodrigues-da-Silva, R. N., da Silva Soares, I., da Costa Lima-Junior, J., et al.**, Apical membrane protein 1-specific antibody profile and temporal changes in peripheral blood B-cell populations in *Plasmodium vivax* malaria. *Parasite Immunol.* 2019. **41**: e12662.

30 **Zaimoku, Y., Patel, B. A., Kajigaya, S., Feng, X., Alemu, L., Quinones Raffo, D., Groarke, E. M., et al.**, Deficit of circulating CD19(+) CD24(hi) CD38(hi) regulatory B cells in severe aplastic anaemia. *Br. J. Haematol.* 2020. **190**: 610–617.

31 **Han, X., Yang, J., Zhang, Y., Zhang, Y., Cao, H., Cao, Y. and Qi, Z.**, Potential role for regulatory B cells as a major source of interleukin-10 in spleen from *Plasmodium chabaudi*-infected mice. *Infect. Immun.* 2018. **86**: e00016-18.

32 **Kalkal, M., Chauhan, R., Thakur, R. S., Tiwari, M., Pande, V. and Das, J.**, IL-10 producing regulatory B cells mediated protection against murine malaria pathogenesis. *Exp. Biol. Med. (Basel)* 2022. **11**: 669.

33 **Liu, Y., Chen, Y., Li, Z., Han, Y., Sun, Y., Wang, Q., Liu, B., et al.**, Role of IL-10-producing regulatory B cells in control of cerebral malaria in *Plasmodium berghei* infected mice. *Eur. J. Immunol.* 2013. **43**: 2907–2918.

34 **Soares, R. R., Antinarelli, L. M. R., Abramo, C., Macedo, G. C., Coimbra, E. S. and Scopel, K. K. G.**, What do we know about the role of regulatory B cells (Breg) during the course of infection of two major parasitic diseases, malaria and leishmaniasis? *Pathog. Glob. Health* 2017. **111**: 107–115.

35 **Takenaka, M. C., Robson, S. and Quintana, F. J.**, Regulation of the T cell response by CD39. *Trends Immunol.* 2016. **37**: 427–439.

36 **Figueiro, F., Muller, L., Funk, S., Jackson, E. K., Battastini, A. M. and Whiteside, T. L.**, Phenotypic and functional characteristics of CD39(high) human regulatory B cells (Breg). *Oncoimmunology* 2016. **5**: e1082703.

37 **Huang, Y., Chen, Z., Wang, H., Ba, X., Shen, P., Lin, W., Wang, Y., et al.**, Follicular regulatory T cells: a novel target for immunotherapy? *Clin. Transl. Immunol.* 2020. **9**: e1106.

38 **Crotty, S. and Follicular T.**, Helper cell biology: a decade of discovery and diseases. *Immunity* 2019. **50**: 1132–1148.

39 **Sage, P. T., Paterson, A. M., Lovitch, S. B. and Sharpe, A. H.**, The coinhibitory receptor CTLA-4 controls B cell responses by modulating T follicular helper, T follicular regulatory, and T regulatory cells. *Immunity* 2014. **41**: 1026–1039.

40 **Wing, J. B., Ise, W., Kurosaki, T. and Sakaguchi, S.**, Regulatory T cells control antigen-specific expansion of Tfh cell number and humoral immune responses via the coreceptor CTLA-4. *Immunity* 2014. **41**: 1013–1025.

41 **Fonseca, V. R., Agua-Doce, A., Maceiras, A. R., Pierson, W., Ribeiro, F., Romao, V. C., Pires, A. R., et al.**, Human blood Tfr cells are indicators of ongoing humoral activity not fully licensed with suppressive function. *Sci. Immunol.* 2017. **2**: eaan1487.

42 **Obeng-Adjei, N., Portugal, S., Holla, P., Li, S., Sohn, H., Ambegaonkar, A., Skinner, J., et al.**, Malaria-induced interferon-gamma drives the expansion of Tbethi atypical memory B cells. *PLoS Pathog.* 2017. **13**: e1006576.

43 **Chan, J. A., Loughland, J. R., de la Parte, L., Okano, S., Ssewanyana, I., Nalubega, M., Nankya, F., et al.**, Age-dependent changes in circulating Tfh cells influence development of functional malaria antibodies in children. *Nat. Commun.* 2022. **13**: 4159.

44 **Oyong, D. A., Loughland, J. R., Soon, M. S. F., Chan, J. A., Andrew, D., Wines, B. D., Hogarth, P. M., et al.**, Adults with *Plasmodium falciparum* malaria have higher magnitude and quality of circulating T-follicular helper cells compared to children. *E. Bio. Med.* 2022. **75**: 103784.

45 **Rosser, E. C. and Mauri, C.**, Regulatory B cells: Origin, phenotype, and function. *Immunity* 2015. **42**: 607–612.

46 **Flores-Borja, F., Bosma, A., Ng, D., Reddy, V., Ehrenstein, M. R., Isenberg, D. A. and Mauri, C.**, CD19+CD24hiCD38hi B cells maintain regulatory T cells while limiting TH1 and TH17 differentiation. *Sci. Transl. Med.* 2013. **5**: 173ra123.

47 **Reis, I. C., Honorio, N. A., Barros, F. S., Barcellos, C., Kitron, U., Camara, D. C., Pereira, G. R., et al.**, Epidemic and endemic malaria transmission related to fish farming ponds in the amazon frontier. *PLoS One* 2015. **10**: e0137521.

48 **Ladeia-Andrade, S., Menezes, M. J., de Sousa, T. N., Silvino, A. C. R., de Carvalho, J. F. Jr., Salla, L. C., Nery, O. A., et al.**, Monitoring the efficacy of chloroquine-primaquine therapy for uncomplicated *Plasmodium vivax* malaria in the main transmission hot spot of Brazil. *Antimicrob. Agents Chemother.* 2019. **63**: e01965-18.

49 **Vicentin, E. C., Francoso, K. S., Rocha, M. V., Iourtov, D., Dos Santos, F. L., Kubrusly, F. S., Sakauchi, M. A., et al.**, Invasion-inhibitory antibodies elicited by immunization with *Plasmodium vivax* apical membrane antigen-1 expressed in *Pichia pastoris* yeast. *Infect. Immun.* 2014. **82**: 1296–1307.

50 **Cunha, M. G., Rodrigues, M. M. and Soares, I. S.**, Comparison of the immunogenic properties of recombinant proteins representing the *Plasmodium vivax* vaccine candidate MSP1(19) expressed in distinct bacterial vectors. *Vaccine* 2001. **20**: 385–396.

Abbreviations: **API**: annual parasite incidence · **ICOS**: inducible costimulator · **MSP1**: merozoite surface protein 1

Full correspondence: Dr. Silvia B. Boscardin and Dr. Marcelo U. Ferreira, Institute of Biomedical Sciences, University of São Paulo, Av. Prof. Lineu Prestes 1374, 05508-000, SP, Brazil
e-mail: sbboscardin@usp.br and muferrei@usp.br

Received: 4/1/2023
Revised: 10/4/2023
Accepted: 8/5/2023
Accepted article online: 9/5/2023